ADVANCED QUANTUM TECHNOLOGIES
www.advquantumtech.com

Bright Source of Purcell-Enhanced, Triggered, Single Photons in the Telecom C-Band

Cornelius Nawrath, Raphael Joos,* Sascha Kolatschek, Stephanie Bauer, Pascal Pruy, Florian Hornung, Julius Fischer, Jiasheng Huang, Ponraj Vijayan, Robert Sittig, Michael Jetter, Simone Luca Portalupi, and Peter Michler*

Several emission features mark semiconductor quantum dots as promising non-classical light sources for prospective quantum implementations. For long-distance transmission and Si-based on-chip processing, the possibility to match the telecom C-band is decisive, while source brightness and high single-photon purity are key features in virtually any quantum implementation. An InAs/InGaAs/GaAs quantum dot emitting in the telecom C-band coupled to a circular Bragg grating is presented here. This cavity structure stands out due to its high broadband collection efficiency and high attainable Purcell factors. Here, simultaneously high brightness with a fiber-coupled single-photon count rate of 13.9 MHz for an excitation repetition rate of 228 MHz (first-lens single-photon collection efficiency ≈17% for NA = 0.6), while maintaining a low multi-photon contribution of $g^{(2)}(0) = 0.0052$ is demonstrated. Moreover, the compatibility with temperatures of up to 40 K attainable with compact cryo coolers, further underlines the suitability for out-of-the-lab implementations.

1. Introduction

Efficient on-demand sources of single photons have a number of applications ranging from quantum communication[1–3] and cryptography[2,3] to metrology.[4] An emission wavelength in the telecom C-band (1530–1565 nm) is especially sought-after due to the compatibility with the mature silicon photonics platform,[5,6] as well as for both free space (low solar background and Rayleigh scattering),[7] and fiber-based transmission (absorption minimum and low dispersion).

Among non-classical light emitters around 1550 nm,[8] semiconductor quantum dots (QDs) on InP have been investigated for two decades,[1,9–17] culminating in application-oriented implementations such as quantum key distribution over 120 km of fiber,[1] teleportation of time-bin qubits,[15] and distribution of single photons, and entangled photon pairs over 4.6 km of deployed fiber.[14] More recently, InAs/GaAs QDs have gained increasing interest, as the material system is widespread in research and industry due to its low cost and well-developed processing techniques. To alleviate the strain between InAs and GaAs, which limits the emission of the current state-of-the-art QDs to the near-infrared regime, metamorphic buffer layers (MMBs)[18–20] have been employed, enabling operation in the telecom C-band and opening the route for a number of studies mainly on the fundamental properties for quantum applications, that is single-photon emission,[19,21–23] entangled photon pair emission,[22,24,25] and photon indistinguishability.[21,23] More recently, this type of source has been used to distribute random numbers in a metropolitan area fiber network.[26]

While the feasibility of device integration as an advantage of the solid-state environment has been exploited around 1550 nm,[13,14] few studies report on tackling the related brightness limitation due to total internal reflection. For the InP material system mesas,[16,17] optical horn structures,[1,9,11] and photonic crystal cavities[10,12] have been reported, claiming up to 13.3% of collection efficiency into the first lens (NA = 0.4).[16] For GaAs-based QDs, the recently reported efficient MMB design[20] compatible with an optical thickness of λ in growth direction, has opened the possibility for the incorporation into high-quality photonic structures.[20,27]

Among the possible implementations of such cavities, the circular Bragg grating (CBG)[28–30] offers the simultaneous advantage of Purcell enhancement of the radiative decay, as well as a broadband increase of the collection efficiency. With this, CBGs are capable of simultaneously supporting both transitions of

C. Nawrath, R. Joos, S. Kolatschek, S. Bauer, P. Pruy, F. Hornung, J. Fischer[+], J. Huang, P. Vijayan, R. Sittig, M. Jetter, S. L. Portalupi, P. Michler
Institut für Halbleiteroptik und Funktionelle Grenzflächen (IHFG), Center for Integrated Quantum Science and Technology (IQST) and SCoPE
University of Stuttgart
70569 Stuttgart, Germany
E-mail: c.nawrath@ihfg.uni-stuttgart.de; r.joos@ihfg.uni-stuttgart.de

The ORCID identification number(s) for the author(s) of this article can be found under https://doi.org/10.1002/qute.202300111

[+]Present address: QuTech and Kavli Institute of Nanoscience, Delft University of Technology, Delft 2628 CJ, Netherlands

DOI: 10.1002/qute.202300111

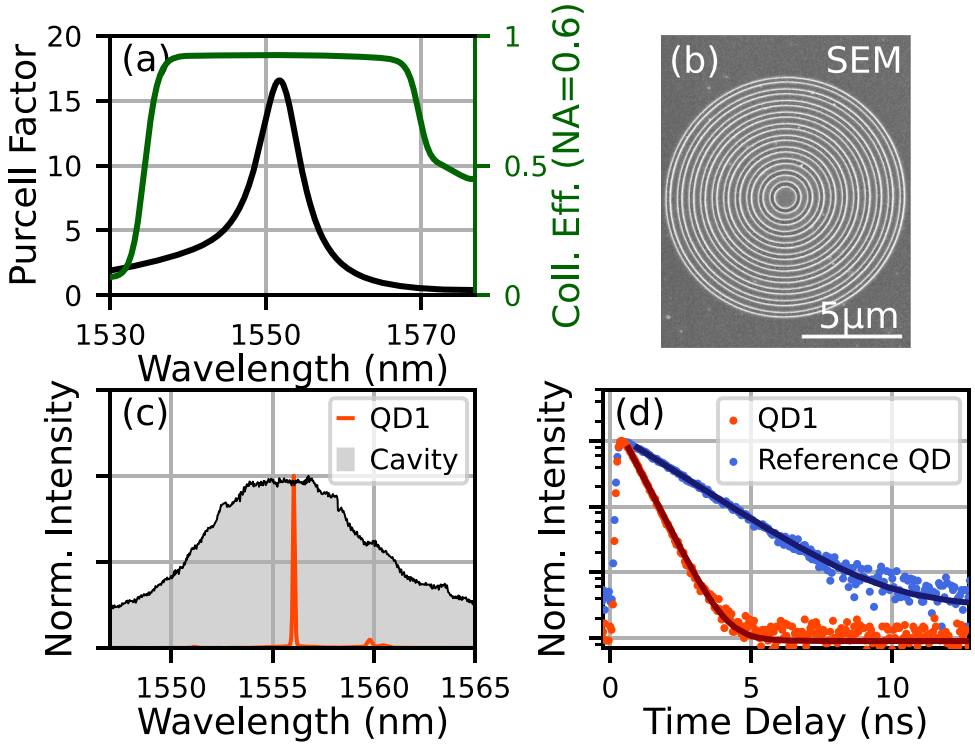

Figure 1. CBG characterization: a) FDTD simulations for Purcell factor and collection efficiency (NA = 0.6). b) SEM image of the CBG. c) Spectrum of the cavity mode under cw non-resonant pumping (9.5 µW) and of QD1 under p-shell excitation. d) TCSPC measurements with fits (solid lines) under non-resonant excitation at 850 nm of QD1 (decay time 0.52 ns) and a reference QD (decay time 1.59 ns) in a semi-logarithmic scale.

the biexciton-exciton cascade, generating polarization-entangled photon pairs. [29,30] CBGs have been reported for the telecom O-band[31–33] and the design parameters have been investigated by simulations for the GaAs and InP system[27,34] for the telecom C-band, however, an experimental realization had yet to be demonstrated.

Here, we close this gap, investigating an InAs/InGaAs/GaAs QD emitting in the telecom C-band incorporated into a non-deterministically placed CBG, reaching a Purcell enhancement of a factor of (3.0 ± 0.7). The device combines a simultaneously high first-lens single-photon collection efficiency of (17.4 ± 0.9)% (NA = 0.6) and a single-photon count rate of 4.77 × 10^6 s^{-1} at 76 MHz repetition rate (end-to-end-efficiency of 6.3%) coupled to a single-mode fiber, with a low multi-photon contribution ($g^{(2)}_{\text{analyt}}(0)$ = (7.2 ± 4.0) × 10^{-3}). We further demonstrate the thermal stability of these properties up to temperatures attainable with compact cryocoolers: at 40 K a count rate of 2.96 × 10^6 s^{-1} is achieved with $g^{(2)}_{\text{analyt}}(0) = (4.32 \pm 0.13) \times 10^{-2}$. Repetition rates up to 228 MHz are investigated, showing that the Purcell factor of (3.0 ± 0.7) allows to maintain high brightness and purity values (fiber-coupled single-photon court rate FCSPCR = 13.88×10^6 s^{-1}, $g^{(2)}_{\text{analyt}}(0) = (5.2 \pm 0.1) \times 10^{-3}$ at 228 MHz). To the best of our knowledge, this FCSPCR exceeds highest value reported for a QD-based single-photon source in the telecom C-band by around two orders of magnitude,[16] while more than a factor of four is found including results in the telecom L-band.[1] Finally, we measure the two-photon interference (TPI) visibility of the emission.

2. Results and Discussion

2.1. Device Characterization

The sample is based on the recently reported thin MMB design and corresponding QD growth optimizations.[20] The device fabrication[31] employs a flip-chip process, to transfer the sample to a Si carrier. The CBG structure is realized by a combination of wet chemical etching, electron beam lithography, and ICP-RIE etching. For details refer to the Supporting Information.

The optimal wavelength dependent performance of the device (see Supporting Information for details) is investigated via finite-difference time-domain (FDTD) simulations as presented in **Figure 1**a, assuming the QD to be placed perfectly in the center of the CBG structure. The collection efficiency (NA = 0.6) is above 85% for almost the entire telecom C-band, with maximum values of more than 92%. Geometrical brightness enhancement in combination with the maximum Purcell factor of 16.6 (FWHM = 7.45 nm, quality factor (Q-factor = 208)) makes this device design appealing for bright emission of single photons and entangled photon pairs.[29,30]

A scanning electron microscopy (SEM) image of the finished device can be seen in Figure 1b. The cavity mode, taken as the spectrum under continuous-wave (cw) non-resonant pumping[35] with an excitation power of 9.5µW (shaded curve in Figure 1c) exhibits a FWHM of (9.74 ± 1.8) nm (Q-factor (160^{+25}_{-36})) and is in good agreement with the mode expected from the FDTD simulations. The slightly larger width is in part due to a minor ellipticity, leading to a polarization mode splitting of (1.24 ± 0.03) nm. This

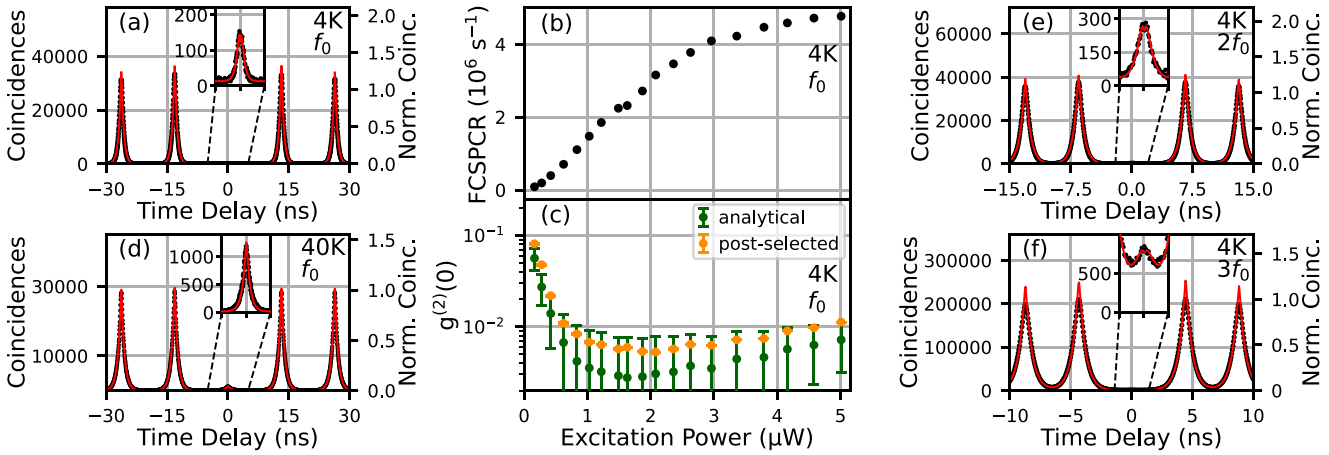

Figure 2. Brightness and single-photon purity of QD1 under p-shell excitation: a) $g^{(2)}(\tau)$ at 4 K, $P = 5.01\,\mu$W and $f_0 = 76$ MHz. b,c) fiber-coupled single-photon count rate (FCSPCR) after the full setup at the detector, corrected for the detection efficiency of 85%, and $g^{(2)}(0)$ over the excitation power. d) $g^{(2)}(\tau)$ at 40 K and $P = 5.01\,\mu$W. e,f) $g^{(2)}(\tau)$ at 4 K, $P = 10.02\,\mu$W, $2f_0 = 152$ MHz, and $P = 15.03\,\mu$W, $3f_0 = 228$ MHz, respectively. Exemplary spectra under these measurement conditions are provided in the Supporting Information.

is estimated to correspond to an elongation of the central disk of ≈1 nm in one direction.

The investigated QD transition, abbreviated as QD1 from here on, (solid orange line in Figure 1c), in spectral resonance with the cavity mode is excited via its p-shell ≈1530 nm. We attribute this transition to a positively charged trion. Note that other QD candidates with similar properties are found on the same sample. An approximate yield of such promising candidates for this non-deterministically placed CBG fabrication is ≈0.05% while devices with QD transition lines matching the cavity mode are found with a yield of ≈0.5%. Details on the optical setup and measurement methods can be found in the Supporting Information.

Time-correlated single-photon counting (TCSPC) measurements of the decay time as displayed in Figure 1d, yield a value of 0.52 ns for QD1 and a mean value of 1.55 ns (standard deviation 0.37 ns) for six exemplary trion transitions of QDs on the same sample outside of CBG structures. This results in a Purcell factor of (3.0 ± 0.7). The discrepancy between the maximally expected and the measured value is attributed mainly to a spatial offset between the center of the non-deterministically positioned CBG and the QD (see Supporting Information). Deterministic fabrication methods[29,36] promise to bring the experimental value close to its optimum, benefitting the attainable transmission rates in quantum communication applications.[14]

2.2. Single-Photon Purity and Brightness Evaluation

Key figures of merit of such schemes are the brightness and the single-photon purity.[1,3] The latter is evaluated via the second-order auto-correlation function $g^{(2)}(\tau)$, for different excitation powers P. **Figure 2**a shows an exemplary measurement result and fit function (solid line) at an excitation power $P = 5.01\,\mu$W measured above the objective. For the normalization and evaluation, bunching processes up to the millisecond time scale are taken into account. The significantly suppressed peak at zero time delay exhibits a dip that is attributed to a slight refilling from the QD surrounding, for example, via charge carrier trap states. The fit function takes this feature into account and upon fully analytical evaluation excluding any offset on the ordinal, a value as low as $g^{(2)}_{\text{analyt}}(0) = (7.2 \times 4.0) \times 10^{-3}$ is found. As for applications any coincidences from background contributions are also relevant, the corresponding post-selected value $g^{(2)}_{\text{ps}}(0) = 1.12 \times 10^{-2}$ is evaluated in the full repetition period of ±6.58 ns, corrected for coincidences from detector dark counts (see Supporting Information for details on purity evaluations and a discussion of the influence of the post-selection window on $g^{(2)}_{\text{ps}}(0)$). Based on these results, a value of $g^{(2)}_{\text{ps}}(0) < 0.5$ can conservatively be estimated even at repetition rates exceeding 1 GHz.

Notably, we find only a minor trade-off between this high single-photon purity and the brightness: Figure 2b,c displays the FCSPCR at the detector, including corrections for dark counts, multi-photon contribution and detection efficiency, and the corresponding values for $g^{(2)}(0)$ over the excitation power. The slightly reduced purity values for low excitation powers are attributed to a power-dependent change in the charge carrier environment of the QD possibly connected to increased refilling or the influence of a second QD. The influence of the charge carrier environment is further investigated via power-dependent measurements with additional weak, non-resonant illumination as presented in the Section SXIV, Supporting Information. This is evidenced by a decrease of blinking behavior especially at low pumping powers. For $P = 5.01\,\mu$W, a value of FCSPCR $= 4.77 \times 10^6$ s^{-1} (raw, detected count rate 3.91×10^6 s^{-1}) is found (see Supporting Information for details). This corresponds to an end-to-end efficiency of 6.3% and a single-photon collection efficiency of (17.4 ± 0.9)% into the first optical element (NA= 0.6) (see Supporting Information). Note that due to the observed blinking, the source is active ≈70% of the time at saturation (see Supporting Information). Integrating the QD in a diode structure is expected to eliminate this limitation.[37] Further effects that may limit this value are a deviation of the spatial cavity mode profile from an ideal Gaussian far-field emission mode, limiting the fiber-coupling efficiency and thus the measured brightness on the employed fiber-coupled detectors. Furthermore, a possible

Table 1. Overview over the brightness and single-photon purity measures determined for QD1 under different p-shell excitation conditions in saturation.

	4 K, 76 MHz	4 K, 228 MHz	40 K, 76 MHz
$g^{(2)}_{\text{analyt}}(0)$	$(7.2 \pm 0.4) \times 10^{-3}$	$(5.2 \pm 0.1) \times 10^{-3}$	$(4.32 \pm 0.13) \times 10^{-2}$
$g^{(2)}_{\text{pst}}(0)$	1.12×10^{-2}	2.32×10^{-2}	4.89×10^{-2}
FCSPCR	$4.77 \times 10^6\ \text{s}^{-1}$	$13.88 \times 10^6\ \text{s}^{-1}$	$2.96 \times 10^6\ \text{s}^{-1}$
collection efficiency	$(17.4 \pm 0.9)\%$	$(16.9 \pm 0.9)\%$	$(11.0 \pm 0.6)\%$
End-to-end efficiency	6.3%	6.1%	3.9%

non-unity state preparation fidelity may pose a limitation.[21,23] However, also in the current state the presented device outperforms all QD emitters with emission around the C-band, reported so far: even with sophisticated structures on the well-established InP material basis,[1,9,11,16,17] 13.3% of first-lens collection efficiency[17] have not been surpassed. Apart from this purely source-related measure, the efficiency of the collection and filtering determines the usable count rate in applications, but has rarely been reported with high values[1,9,11] (record end-to-end efficiency around 1550 nm so far in the telecom L-band: 5%[1]). The presented work thus signifies an important advance toward out-of-the-lab implementations.

Moreover, the device exhibits a very notable degree of stability regarding brightness and purity at elevated temperatures:[31,38] the measurement of $g^{(2)}(\tau)$ at a temperature of 40 K and $P = 5.01\,\mu\text{W}$, as displayed in Figure 2d, results in values of $g^{(2)}_{\text{analyt}}(0) = (4.32 \pm 0.13) \times 10^{-2}$ and $g^{(2)}_{\text{ps}}(0) = 4.89 \times 10^{-2}$. A maximum of FCSPCR $= 2.96 \times 10^6\ \text{s}^{-1}$ (raw, detected count rate $2.47 \times 10^6\ \text{s}^{-1}$) is found. This temperature stability allows the implementation in compact and economic Stirling cryocoolers.[39]

A further decisive advantage is the Purcell-enhanced decay time. It allows for higher excitation repetition rates, while maintaining high single-photon purity. Figure 2e,f displays measurements of $g^{(2)}(\tau)$ at 152 and 228 MHz repetition rate, 4 K and the same excitation power per pulse as the measurements displayed in Figure 2a,b. Values of $g^{(2)}_{\text{analyt}} = (1.08 \pm 0.56) \times 10^{-2}$ ($g^{(2)}_{\text{ps}} = 1.51 \times 10^{-2}$), and $g^{(2)}_{\text{analyt}} = (5.2 \pm 0.1) \times 10^{-3}$ ($g^{(2)}_{\text{ps}} = 2.32 \times 10^{-2}$) are found, respectively (see Supporting Information for further measurements). The corresponding maximum values FCSPCR $= 9.44 \times 10^6\ \text{s}^{-1}$ (raw, detected countrate $7.75 \times 10^6\ \text{s}^{-1}$) and FCSPCR $= 13.88 \times 10^6\ \text{s}^{-1}$ (raw, detected countrate $11.37 \times 10^6\ \text{s}^{-1}$), respectively, further underline the suitability of the source for applications. Note that especially at high repetition rates, due to the overlap of the peaks, a slight reduction of the post-selection window further decreases $g^{(2)}_{\text{ps}}(0)$ while maintaining a high count rate (see Supporting Information).

Table 1 provides a summary over the different brightness and single-photon purity measurements under p-shell excitation for QD1.

2.3. Two-Photon Interference Visibility

For a large number of implementations,[1,3] high brightness and purity are the only requirements. Nonetheless, here we benchmark the photon coherence which is of importance in other applications.[15,40,41] To this end, the degree of indistinguishability (TPI visibility, V_{TPI}) of photons emitted 6.6 ns apart is probed. An exemplary correlation at $P = 7.7\,\mu\text{W}$ for the measurements with parallel and orthogonal (completely distinguishable) polarization is displayed in **Figure 3**a alongside the respective fits. Note that the evaluations of V_{TPI} are extracted from the parallel data set as slight fluctuations of the bunching parameters between measurement runs are found to render this self-consistent method more reliable than a comparison with the orthogonal case. In the displayed case, however, the discrepancy is negligible and the orthogonal measurement is displayed as a guide to the eye. The partial suppression of the central peak for parallel polarization results in a value of $V_{\text{TPI,analyt}} = (8.10 \pm 3.38)\%$. Little dependence of V_{TPI} (see Supporting Information for corresponding linewidth values) on the excitation power is found, as is shown in Figure 3b for the values via analytical and post-selected evaluation. Despite the Purcell enhancement of the decay rate, these results are comparable to V_{TPI} found under purely resonant excitation for a QD with only a bottom DBR.[23] Note, however, that in the latter case the signal was filtered to 5 GHz (see Supporting Information for further measurements and discussions). Instabilities of the magnetic[42,43] or electric field[42,44] at the site of the QD are assumed to be responsible for the decoherence of the emission. Ref. [36] suggests that the proximity to the surface should not influence the emission for the device dimensions. Thus, the stabilization of the magnetic[42,43] and electric field,[42,44] is expected

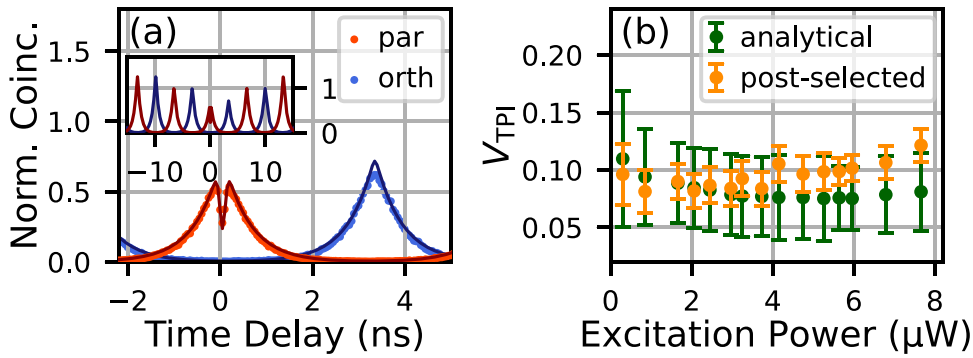

Figure 3. TPI visibility of QD1 under p-shell excitation: a) exemplary TPI measurement for parallel (par) and orthogonal (orth) polarization at $P = 7.7\,\mu\text{W}$. The orthogonal data and fit are offset horizontally for visual clarity. b) V_{TPI} for different excitation powers.

to improve the coherence more than the application of a passivation layer.[36] Such implementations promise to combine the high brightness and purity of the emission with a high degree of photon indistinguishability, further broadening the range of possible applications.

3. Conclusion

In summary, a bright source of single photons in the telecom C-band based on an InAs/InGaAs/GaAs QD under p-shell excitation in a circular Bragg grating is presented. A simultaneously high fiber-coupled single-photon count rate of 13.88 MHz for an excitation repetition rate of 228 MHz (first-lens single-photon collection efficiency $\approx$ (17.4±0.9)% for NA = 0.6) is demonstrated while maintaining a low multi-photon contribution of $g^{(2)}_{\mathrm{analyt}}(0) = (5.2 \pm 0.1) \times 10^{-3}$ due to the Purcell factor of (3.0 ± 0.7). Furthermore, compatibility with compact cryocoolers is demonstrated, opening routes for real-world implementations. Finally, the degree of indistinguishability is investigated, identifying possible strategies to improve the coherence of the emission. A combination of this approach with deterministic fabrication methods, the integration into an electrically gated structure, or the application of a passivation layer, are expected to further boost the Purcell factor, brightness, and coherence of the emission significantly.

Note added in proof: During the review process for the work at hand, Holewa et al. have presented an investigation on deterministically placed CBG structures with pre-selected InAs/InP QDs emitting in the telecom C-band.[45] This fabrication method allows for a notable yield of ≈30% of promising QD-CBG structures. The attained optical quality of the emission is comparable to the values presented in the work at hand regarding Purcell factor and indistinguishability. However, in contrast to the results presented here, the authors find a major trade-off between brightness and purity: appealing collection efficiencies of up to 16.6% into a small NA of 0.4 are demonstrated under non-resonant excitation in saturation, however, in connection with a reduced purity values on the order of $g^{(2)}(0) > 0.1$. Improved purity values are found for quasi-resonant excitation but no evaluation of the corresponding brightness is presented.

Supporting Information

Supporting Information is available from the Wiley Online Library or from the author.

Acknowledgements

C.N. and R.J. contributed equally to this work. The authors want to thank Philipp Flad and Monika Ubl for their help and acknowledge the companies Single Quantum and PriTel Inc. for the persistent and timely support. The authors gratefully acknowledge funding by the German Federal Ministry of Education and Research (BMBF) via the project QR.X (No.16KISQ013) and the European Union's Horizon 2020 research and innovation program under Grant Agreement No. 899814 (Qurope). Furthermore, this project (20FUN05 SEQUME) has received funding from the EMPIR programme co-financed by the Participating States and from the European Union's Horizon 2020 research and innovation programme. This work was also funded by the Deutsche Forschungsgemeinschaft (DFG, German Research Foundation) - 431314977/GRK2642 and the Quantum Technology BW via the project TelecomSPS.

Open access funding enabled and organized by Projekt DEAL.

Conflict of Interest

The authors declare no conflict of interest.

Data Availability Statement

The data that support the findings of this study are available from the corresponding author upon reasonable request.

Keywords

circular Bragg cavity, Purcell effect, quantum dot, single photon, telecom C-band

Received: April 27, 2023
Revised: August 7, 2023
Published online: August 31, 2023

[1] K. Takemoto, Y. Nambu, T. Miyazawa, Y. Sakuma, T. Yamamoto, S. Yorozu, Y. Arakawa, *Sci. Rep.* **2015**, *5*, 14383.
[2] F. Xu, X. Ma, Q. Zhang, H.-K. Lo, J.-W. Pan, *Rev. Mod. Phys.* **2020**, *92*, 025002.
[3] M. Bozzio, M. Vyvlecka, M. Cosacchi, C. Nawrath, T. Seidelmann, J. C. Loredo, S. L. Portalupi, V. M. Axt, P. Michler, P. Walther, *npj Quantum Inf.* **2022**, *8*, 104.
[4] H. Georgieva, M. López, H. Hofer, N. Kanold, A. Kaganskiy, S. Rodt, S. Reitzenstein, S. Kück, *Opt. Express* **2021**, *29*, 23500.
[5] X. Qiang, X. Zhou, J. Wang, C. M. Wilkes, T. Loke, S. O'Gara, L. Kling, G. D. Marshall, R. Santagati, T. C. Ralph, J. B. Wang, J. L. O'Brien, M. G. Thompson, J. C. F. Matthews, *Nat. Photonics* **2018**, *12*, 534.
[6] S. Bauer, D. Wang, N. Hoppe, C. Nawrath, J. Fischer, N. Witz, M. Kaschel, C. Schweikert, M. Jetter, S. L. Portalupi, M. Berroth, P. Michler, *Appl. Phys. Lett.* **2021**, *119*, 211101.
[7] S.-K. Liao, H.-L. Yong, C. Liu, G.-L. Shentu, D.-D. Li, J. Lin, H. Dai, S.-Q. Zhao, B. Li, J.-Y. Guan, W. Chen, Y.-H. Gong, Y. Li, Z.-H. Lin, G.-S. Pan, J. S. Pelc, M. M. Fejer, W.-Z. Zhang, W.-Y. Liu, J. Yin, J.-G. Ren, X.-B. Wang, Q. Zhang, C.-Z. Peng, J.-W. Pan, *Nat. Photonics* **2017**, *11*, 509.
[8] X. Cao, M. Zopf, F. Ding, *J. Semicond.* **2019**, *40*, 071901.
[9] K. Takemoto, M. Takatsu, S. Hirose, N. Yokoyama, Y. Sakuma, T. Usuki, T. Miyazawa, Y. Arakawa, *J. Appl. Phys.* **2007**, *101*, 081720.
[10] M. D. Birowosuto, H. Sumikura, S. Matsuo, H. Taniyama, P. J. van Veldhoven, R. Nötzel, M. Notomi, *Sci. Rep.* **2012**, *2*, 321.
[11] T. Miyazawa, K. Takemoto, Y. Nambu, S. Miki, T. Yamashita, H. Terai, M. Fujiwara, M. Sasaki, Y. Sakuma, M. Takatsu, T. Yamamoto, Y. Arakawa, *Appl. Phys. Lett.* **2016**, *109*, 132106.
[12] A. Kors, K. Fuchs, M. Yacob, J. P. Reithmaier, M. Benyoucef, *Appl. Phys. Lett.* **2017**, *110*, 031101.
[13] T. Müller, J. Skiba-Szymanska, A. B. Krysa, J. Huwer, M. Felle, M. Anderson, R. M. Stevenson, J. Heffernan, D. A. Ritchie, A. J. Shields, *Nat. Commun.* **2018**, *9*, 862.
[14] G. Shooter, Z.-H. Xiang, J. R. A. Müller, J. Skiba-Szymanska, J. Huwer, J. Griffiths, T. Mitchell, M. Anderson, T. Müller, A. B. Krysa, R. Mark Stevenson, J. Heffernan, D. A. Ritchie, A. J. Shields, *Opt. Express* **2020**, *28*, 36838.
[15] M. Anderson, T. Müller, J. Skiba-Szymanska, A. B. Krysa, J. Huwer, R. M. Stevenson, J. Heffernan, D. A. Ritchie, A. J. Shields, *Phys. Rev. Appl.* **2020**, *13*, 054052.
[16] A. Musiał, M. Mikulicz, P. Mrowiński, A. Zielińska, P. Sitarek, P. Wyborski, M. Kuniej, J. P. Reithmaier, G. Sęk, M. Benyoucef, *Appl. Phys. Lett.* **2021**, *118*, 221101.

[17] P. Holewa, A. Sakanas, U. M. Gür, P. Mrowiński, A. Huck, B.-Y. Wang, A. Musiał, K. Yvind, N. Gregersen, M. Syperek, E. Semenova, *ACS Photonics* **2022**, *9*, 2273.
[18] E. S. Semenova, R. Hostein, G. Patriarche, O. Mauguin, L. Largeau, I. Robert-Philip, A. Beveratos, A. Lemàtre, *J. Appl. Phys.* **2008**, *103*, 103533.
[19] M. Paul, F. Olbrich, J. Höschele, S. Schreier, J. Kettler, S. L. Portalupi, M. Jetter, P. Michler, *Appl. Phys. Lett.* **2017**, *111*, 033102.
[20] R. Sittig, C. Nawrath, S. Kolatschek, S. Bauer, R. Schaber, J. Huang, P. Vijayan, P. Pruy, S. L. Portalupi, M. Jetter, P. Michler, *Nanophotonics* **2022**, *11*, 1109.
[21] C. Nawrath, F. Olbrich, M. Paul, S. L. Portalupi, M. Jetter, P. Michler, *Appl. Phys. Lett.* **2019**, *115*, 023103.
[22] K. D. Zeuner, K. D. Jöns, L. Schweickert, C. Reuterskiöld Hedlund, C. Nuñez Lobato, T. Lettner, K. Wang, S. Gyger, E. Schöll, S. Steinhauer, M. Hammar, V. Zwiller, *ACS Photonics* **2021**, *8*, 2337.
[23] C. Nawrath, H. Vural, J. Fischer, R. Schaber, S. L. Portalupi, M. Jetter, P. Michler, *Appl. Phys. Lett.* **2021**, *118*, 244002.
[24] F. Olbrich, J. Höschele, M. Müller, J. Kettler, S. L. Portalupi, M. Paul, M. Jetter, P. Michler, *Appl. Phys. Lett.* **2017**, *111*, 133106.
[25] T. Lettner, S. Gyger, K. D. Zeuner, L. Schweickert, S. Steinhauer, C. Reuterskiöld Hedlund, S. Stroj, A. Rastelli, M. Hammar, R. Trotta, K. D. Jöns, V. Zwiller, *Nano Lett.* **2021**, *21*, 10501.
[26] S. Gyger, K. D. Zeuner, T. Lettner, S. Bensoussan, M. Carlnäs, L. Ekemar, L. Schweickert, C. R. Hedlund, M. Hammar, T. Nilsson, J. Almlöf, S. Steinhauer, G. V. Llosera, V. Zwiller, *Appl. Phys. Lett.* **2022**, *121*, 194003.
[27] L. Bremer, C. Jimenez, S. Thiele, K. Weber, T. Huber, S. Rodt, A. Herkommer, S. Burger, S. Höfling, H. Giessen, S. Reitzenstein, *Opt. Express* **2022**, *30*, 15913.
[28] L. Sapienza, M. Davanço, A. Badolato, K. Srinivasan, *Nat. Commun.* **2015**, *6*, 7833.
[29] J. Liu, R. Su, Y. Wei, B. Yao, S. F. C. da Silva, Y. Yu, J. Iles-Smith, K. Srinivasan, A. Rastelli, J. Li, X. Wang, *Nat. Nanotechnol.* **2019**, *14*, 586.
[30] H. Wang, H. Hu, T.-H. Chung, J. Qin, X. Yang, J.-P. Li, R.-Z. Liu, H.-S. Zhong, Y.-M. He, X. Ding, Y.-H. Deng, Q. Dai, Y.-H. Huo, S. Höfling, C.-Y. Lu, J.-W. Pan, *Phys. Rev. Lett.* **2019**, *122*, 113602.
[31] S. Kolatschek, C. Nawrath, S. Bauer, J. Huang, J. Fischer, R. Sittig, M. Jetter, S. L. Portalupi, P. Michler, *Nano Lett.* **2021**, *21*, 7740.
[32] S.-W. Xu, Y.-M. Wei, R.-B. Su, X.-S. Li, P.-N. Huang, S.-F. Liu, X.-Y. Huang, Y. Yu, J. Liu, X.-H. Wang, *Photonics Res.* **2022**, *10*, 487440.
[33] A. Barbiero, J. Huwer, J. Skiba-Szymanska, D. J. P. Ellis, R. M. Stevenson, T. Müller, G. Shooter, L. E. Goff, D. A. Ritchie, A. J. Shields, *ACS Photonics* **2022**, *9*, 3060.
[34] A. Barbiero, J. Huwer, J. Skiba-Szymanska, T. Müller, R. M. Stevenson, A. J. Shields, *Opt. Express* **2022**, *30*, 10919.
[35] M. Winger, T. Volz, G. Tarel, S. Portolan, A. Badolato, K. J. Hennessy, E. L. Hu, A. Beveratos, J. Finley, V. Savona, A. Imamoğlu, *Phys. Rev. Lett.* **2009**, *103*, 207403.
[36] J. Liu, K. Konthasinghe, M. Davanço, J. Lawall, V. Anant, V. Verma, R. Mirin, S. W. Nam, J. D. Song, B. Ma, Z. S. Chen, H. Q. Ni, Z. C. Niu, K. Srinivasan, *Phys. Rev. Appl.* **2018**, *9*, 064019.
[37] L. Zhai, M. C. Löbl, G. N. Nguyen, J. Ritzmann, A. Javadi, C. Spinnler, A. D. Wieck, A. Ludwig, R. J. Warburton, *Nat. Commun.* **2020**, *11*, 4745.
[38] C. Carmesin, F. Olbrich, T. Mehrtens, M. Florian, S. Michael, S. Schreier, C. Nawrath, M. Paul, J. Höschele, B. Gerken, J. Kettler, S. L. Portalupi, M. Jetter, P. Michler, A. Rosenauer, F. Jahnke, *Phys. Rev. B* **2018**, *98*, 125407.
[39] A. Schlehahn, S. Fischbach, R. Schmidt, A. Kaganskiy, A. Strittmatter, S. Rodt, T. Heindel, S. Reitzenstein, *Sci. Rep.* **2018**, *8*, 1340.
[40] F. Basso Basset, M. B. Rota, C. Schimpf, D. Tedeschi, K. D. Zeuner, S. F. Covre Da Silva, M. Reindl, V. Zwiller, K. D. Jöns, A. Rastelli, R. Trotta, *Phys. Rev. Lett.* **2019**, *123*, 160501.
[41] M. Zopf, R. Keil, Y. Chen, J. Yang, D. Chen, F. Ding, O. G. Schmidt, *Phys. Rev. Lett.* **2019**, *123*, 160502.
[42] A. V. Kuhlmann, J. H. Prechtel, J. Houel, A. Ludwig, D. Reuter, A. D. Wieck, R. J. Warburton, *Nat. Commun.* **2015**, *6*, 4.
[43] R. N. E. Malein, T. S. Santana, J. M. Zajac, A. C. Dada, E. M. Gauger, P. M. Petroff, J. Y. Lim, J. D. Song, B. D. Gerardot, *Phys. Rev. Lett.* **2016**, *116*, 257401.
[44] A. Reigue, R. Hostein, V. Voliotis, *Semicond. Sci. Technol.* **2019**, *34*, 113001.
[45] P. Holewa, E. Zięba-Ostój, D. A. Vajner, M. Wasiluk, B. Gaál, A. Sakanas, M. Burakowski, P. Mrowiński, B. Krajnik, M. Xiong, A. Huck, K. Yvind, N. Gregersen, A. Musiał, T. Heindel, M. Syperek, E. Semenova, *arXiv:2304.02515*, **2023**.